

XVI. INTERACTION OF LASER RADIATION WITH PLASMAS AND NONADIABATIC MOTION OF PARTICLES IN MAGNETIC FIELDS*

Academic and Research Staff

Prof. D. J. Rose
Prof. T. H. Dupree

Prof. L. M. Lidsky
Prof. S. Yip

Graduate Students

T. S. Brown
J. D. Callen
H. Ching

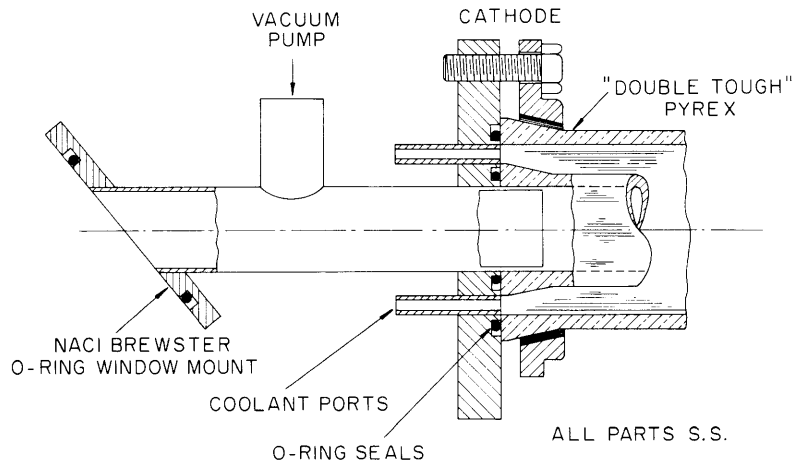
D. E. Crane
M. D. Lubin

R. W. Moir
M. Murakami
A. A. Offenberger

A. INCOHERENT SCATTERING OF LIGHT FROM A PLASMA IV

The N₂-CO₂ laser development for the plasma scattering experiment¹⁻³ has been completed; the optical detecting scheme has been finalized; and, after delivery of a 0.14- μ bandpass filter centered at 10.6 μ , noise measurements were made to determine the NEP of our mercury-doped Ge detector.

The final, and greatly simplified, laser design is indicated in Fig. XVI-1. Two



NOTE: ENDS SYMMETRICAL EXCEPT FOR GAS INLET AND VACUUM PORT SIZES

Fig. XVI-1. Detail of laser discharge tube.

coaxially mounted equal lengths of "Double Tough" Pyrex tubing, 10 ft long and 1 in. and 2 in. I. D., with compressive O-ring sealing to the end flanges, form the discharge region and coolant channel. The flanges incorporate the O-ring mounted NaCl Brewster

*This work was supported by the United States Atomic Energy Commission (Contract AT(30-1)-3285).

(XVI. INTERACTION OF LASER RADIATION WITH PLASMAS)

windows, vacuum fitting and gas inlet ports, cathode and anode for the discharge, and are directly cooled by passing the cooling water through them. The discharge tube and mirrors are mounted on a 4-in. Al H-beam.

The discharge conditions are 100 mA at 12 kV in a gas mixture of 1 Torr CO_2 , 1 Torr N_2 , and 4 Torr He. The mirrors have a separation of 4 m; one being an Au-coated B.S.C. glass, the other a flat Ge mirror. The Au mirror has a 1-mm central hole for alignment purposes when using an He-Ne laser. The Ge mirror, 2-mm thick, has a front surface reflectivity of 36% (index of refraction $n=4$) and the back surface has a ZnS antireflection coating. The output power is ~ 100 watts at 10.59μ , with essential stability on a single rotational transition. At lower power levels, or with slightly detuned mirrors, other rotational lines ($\sim 200 \text{ \AA}$ separation) appear. The output is multi-mode longitudinally and transversely, but this is of no consequence in our scattering experiment. Using a Au-coated mirror with 1-cm hole coupling yields an even higher power level, but does not give the single rotational line stability that the Ge mirror affords. The optics for detecting the scattered radiation from the plasma is indicated in Fig. XVI-2, with the exception of substituting mirrors for lenses in collecting and

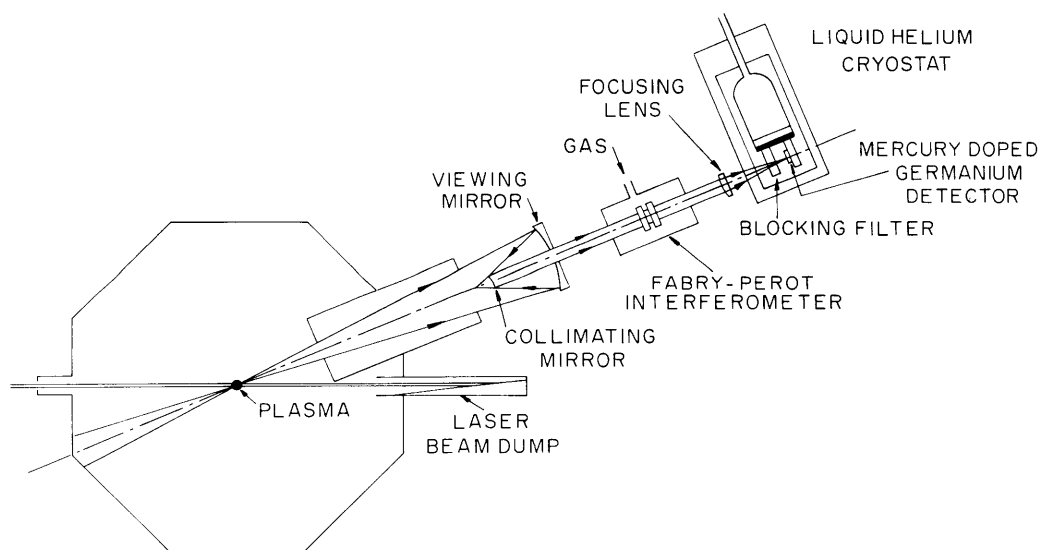


Fig. XVI-2. Laser-plasma scattering-detection optics.

rendering the scattered radiation parallel for wavelength analysis. We found that spherical aberration in the KCl lenses was the limiting factor in utilizing all available scattered light. A redesign, with mirrors substituted for lenses, indicates far less spherical aberration and hence much better collection efficiency. The large mirror subtends $\pi \times 10^{-2}$ sr at the scattering point in the plasma. The mirror assembly

(XVI. INTERACTION OF LASER RADIATION WITH PLASMAS)

is under construction.

The Fabry-Perot interferometer uses Ge plates with 96% ZnS reflective coatings, which affords a 20 Å bandpass. The central wavelength is to be pressure-tuned by using ethane, which will afford a spectral scan of 1400 Å. This range will enable measurement of the plasma-frequency satellite resonances, as well as temperature measurements from the Doppler-shifted intensity spectrum.

An NaCl lens with small spherical aberration focuses the spectrally analyzed radiation onto an Hg-doped Ge detector cooled to 4°K. A Ge substrate blocking filter of 0.14-μ bandpass mounted in the 4°K cryostat blocks all orders from the Fabry-Perot, except one, and additionally limits the 300°K black-body radiation seen by the detector.³ The measured NEP is 2×10^{-14} with a responsivity of 8×10^8 volts watt⁻¹ and watt cps^{-1/2}, source impedance of 1.5 M, compared with an unblocked detector of NEP = 8×10^{-13} watt cps^{-1/2} and responsivity = 2.5×10^6 volt watt⁻¹. A considerable improvement has been achieved. The anticipated scattered power levels are 4×10^{-15} watt; this indicates detection bandwidths of 1/25 cps for a S/N = 1.

The laser radiation is chopped before focusing into the scattering volume, and the scattered signal is detected synchronously by using an FET impedance-matching pre-amplifier and Princeton Applied Research HR-8 lock-in amplifier. The detector noise is well above pre-amplifier noise, and is the limiting factor in this experiment.

The scattered light collecting mirrors are being set up and the only outstanding question will be that of laser beam dump efficiency.

A. A. Offenberger

References

1. A. A. Offenberger, Quarterly Progress Report No. 78, Research Laboratory of Electronics, M.I.T., July 15, 1965, pp. 131-135.
2. A. A. Offenberger, Quarterly Progress Report No. 79, Research Laboratory of Electronics, M.I.T., October 15, 1965, pp. 145-147.
3. A. A. Offenberger, Quarterly Progress Report No. 81, Research Laboratory of Electronics, M.I.T., April 15, 1966, pp. 139-141.

B. ELECTRON DIFFUSION IN THE HELICALLY PERTURBED MAGNETIC FIELD OF THE M.I.T. STELLARATOR

Electrons of 1500 volts are being injected and trapped in a torus for an average of 100 transits. The trapped electrons diffuse outward toward the walls of the torus and are collected in an azimuthally symmetric charge detector. After an initial transient, the current at the collector decays exponentially after the injection current is switched off. This type of behavior implies a random walk of the electrons toward the walls. The

(XVI. INTERACTION OF LASER RADIATION WITH PLASMAS)

average number of transits $N = \frac{R}{\langle(\Delta r)^2\rangle}$, where R is the radius of the vacuum wall, and $\langle(\Delta r)^2\rangle$ is the average square change in the particle's radial position in one transit. $\langle(\Delta r)^2\rangle$ is produced by perturbation fields (waves), as well as gas scattering, scattering from the Stellarator fields in the U-bends, and noncancellation of the toroidal drifts. The perturbing fields are varied while the others are kept as constant as possible; thus their effects can be subtracted out.

The electrons diffuse to the torus in real space, but the perturbing fields produce velocity-space diffusion and almost no real-space diffusion of the guiding centers. The drift cancellation in the U-bends is velocity-dependent and hence converts velocity diffusion into real-space diffusion.

The average number of transits then becomes

$$N = \frac{v_{\perp \text{ loss cone}}^2}{\langle(\Delta v)^2\rangle}$$

in velocity coordinates, where $v_{\perp \text{ loss cone}}$ is the perpendicular (to \vec{B}) velocity at which the electron will be lost rapidly. $\langle(\Delta v_{\perp})^2\rangle$ is the squared change in perpendicular velocity in one transit averaged over all possible initial entrance velocity-space angle (phase average).

The loss cone ($v_{\perp \text{ loss cone}}$) in a torus is not simply defined as in a mirror device, and depends on the drift-cancellation method that is used; however, it does not vary with a change in perturbation field strength, and hence we can measure the dependence of $\langle(\Delta v_{\perp})^2\rangle$ on perturbation field strength, keeping $v_{\perp \text{ loss cone}}$ constant. We plan to measure the loss cone ($v_{\perp \text{ loss}}$), but, at present, we use it as an adjustable parameter to fit the data.

The perturbation field used for this experiment was a static transverse magnetic field rotating in space with a varying pitch length.

A theoretical prediction of the lifetime for weak perturbations is the following.¹

$$N = \left\{ \frac{A \left(\frac{B_{\perp}}{B_0} \right)^2 F(z_0)}{\frac{v_{\perp \text{ loss cone}}^2}{v_0^2}} \right\}^{-1}, \quad (1)$$

where

$$A = \frac{2}{\pi} \frac{LP_0}{a^2 r_0^2}$$

(XVI. INTERACTION OF LASER RADIATION WITH PLASMAS)

$$F(z_0) = \tan \frac{\pi z_0}{2L} \left(1 - a^2 \cos^4 \frac{\pi z_0}{2L} \right)^{3/2}$$

B_0 = field for resonance for 1.5 kV electrons
 = 61.2 Gauss

r_0 = Larmor radius at the resonant field for $v_z = 0$
 = 2.13 cm

a^2 = Percentage of electron energy for which the perturbed field has been
 designed to convert parallel (to \vec{B}) energy to transverse energy (or vice
 versa)
 = 80%

L = length of perturbed-field region = 1 meter

P_0 = resonant pitch length for $v_{\perp} = 0$, = 13.4 cm

z_0 = position at which an electron with $v_{\perp} = 0$ is in resonance for a given B_z ,
 $0 \leq z_0 \leq L$.

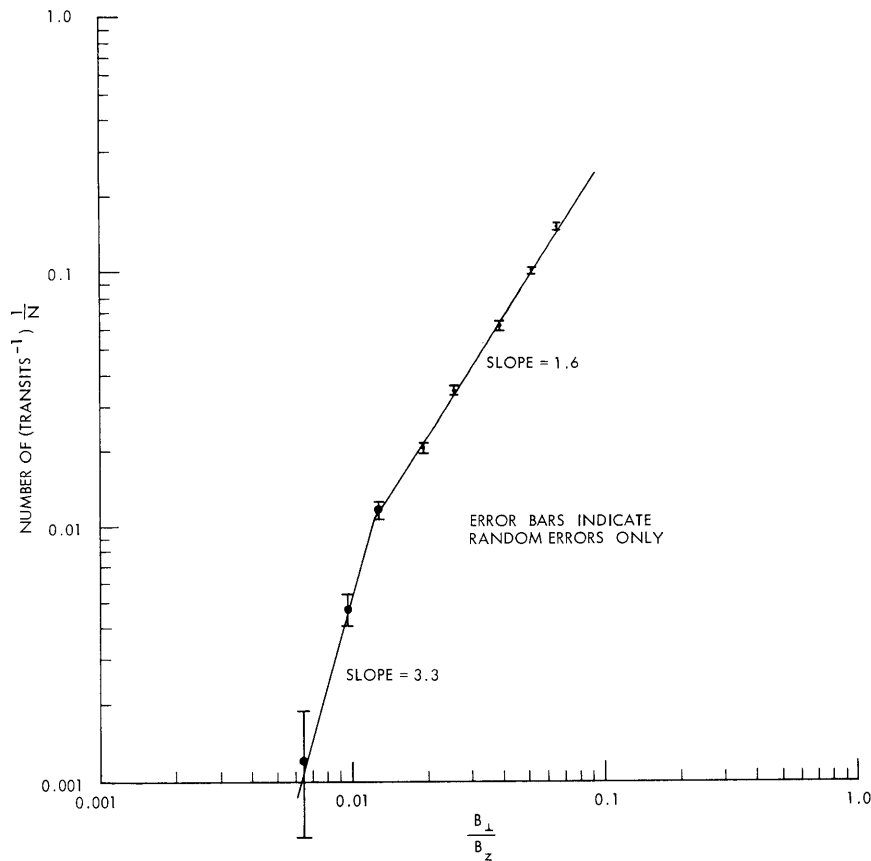


Fig. XVI-3. Diffusion coefficient vs perturbation field strength.

(XVI. INTERACTION OF LASER RADIATION WITH PLASMAS)

The raw data from the experiment was the average number of transits, $N(B_{\perp})$.

$$\frac{1}{N} = \frac{1}{N(B_{\perp})} - \frac{1}{N(o)},$$

where N is the average number of transits attributable to the perturbation field with $N(o) = \infty$.

Figure XVI-3 shows experimental results for Eq. 1, with B_{\perp} varied and all else fixed. Equation 1 predicts a square-law dependence of the number of transits on perturbation field strength. The dependence goes from a 1.6 power law to something higher (possible square law) at fields below $B_{\perp}/B_z = 1.3\%$. The large error bars

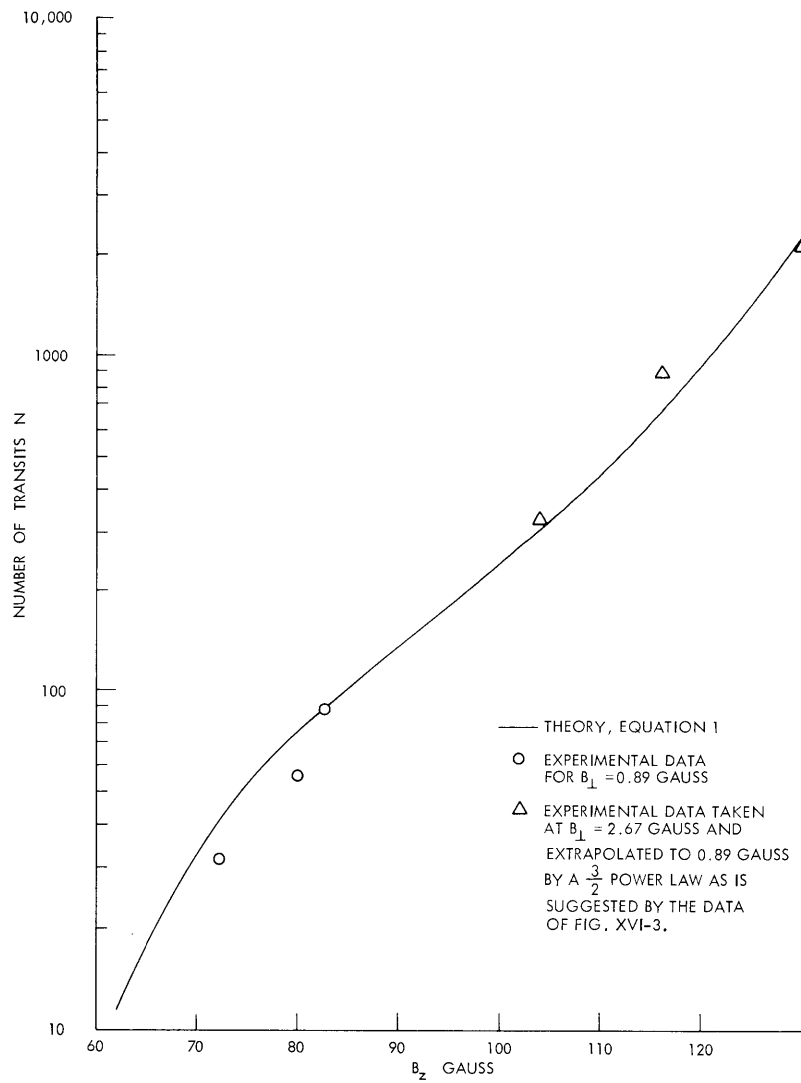


Fig. XVI-4. Lifetime vs magnetic field strength.

(XVI. INTERACTION OF LASER RADIATION WITH PLASMAS)

result from the small difference of large numbers in Eq. 2 for weak perturbation (that is, $N(B_{\perp}) \approx N(0)$).

Clark and Lidsky² predict $N \propto [B^{3/2}]^{-1}$ for sufficiently large B_{\perp} , which is in agreement with the region of Fig. XVI-3 above $B_{\perp}/B_z = 1.3\%$.

The dependence of Eq. 1 on \vec{B} was checked experimentally; it is given in Fig. XVI-4 for a constant value of $B_{\perp} = 0.89$ Gauss. By changing B_z , the resonance point was shifted. $B_z = 61.2$ Gauss corresponds to resonance at the left of Fig. XVI-4 ($z_0 = 100$ cm), while $B_z = 137$ Gauss corresponds to resonance at $z_0 = 0$ for electrons with $v_{\perp} = 0$. An approximate fit to the data was found for $v_{\perp \text{ loss}}/v_0 = 1$.

Researchers have proposed the use of perturbation fields for nonadiabatic traps, whereby molecular ions are trapped by a resonant field. Before that are lost by the inverse trapping process, collisions can break up an appreciable fraction of the molecular ions into atomic ions with half the mass, for instance. Figure XVI-4 gives experimental results that are equivalent to changing the mass of the particles. A molecular ion, H_2^+ say, would behave like an electron in resonance at 61.2 Gauss. An atomic ion of half the mass would be in resonance at 122.4 Gauss and, from Fig. XVI-4, we see that the atomic ion would have a lifetime 100 times longer than the molecular ion. In this perturbed field the pitch changed by more than a factor of 2, so the atomic ion equivalent electrons were still in resonance with a portion of the perturbed field.

During the next quarter we shall investigate diffusion from perturbed fields in the transition region between resonant and nonresonant fields. Also, we plan to measure the size of the loss cone in our torus.

R. W. Moir, L. M. Lidsky

References

1. R. C. Wingerson, T. H. Dupree, and D. J. Rose, Phys. Fluids 7, 1475 (1964); see Eq. (58).
2. L. M. Lidsky, J. F. Clarke, and D. J. Rose, "Experimental and Numerical Investigations of Velocity Diffusion in a Nonadiabatic Injection System," Paper No. 5L-9, Eighth Annual Meeting of the Division of Plasma Physics, Boston, Mass., November 1966; J. F. Clarke and L. M. Lidsky, "Nonclassical Diffusion Produced by a Resonant Helical Magnetic Field Perturbation," Paper No. 51-10; J. F. Clarke, Ph.D. Thesis, Department of Nuclear Engineering, M.I.T., June 1967.

